

Large Extracellular Cord Formation in a Zebrafish Model of Mycobacterium kansasii Infection

Johansen Matt, Kremer Laurent

▶ **To cite this version:**

Johansen Matt, Kremer Laurent. Large Extracellular Cord Formation in a Zebrafish Model of Mycobacterium kansasii Infection. Journal of Infectious Diseases, 2020, pp.jiaa187. 10.1093/infdis/jiaa187 . inserm-02868836

HAL Id: inserm-02868836

https://inserm.hal.science/inserm-02868836

Submitted on 15 Jun 2020

HAL is a multi-disciplinary open access archive for the deposit and dissemination of scientific research documents, whether they are published or not. The documents may come from teaching and research institutions in France or abroad, or from public or private research centers.

L'archive ouverte pluridisciplinaire **HAL**, est destinée au dépôt et à la diffusion de documents scientifiques de niveau recherche, publiés ou non, émanant des établissements d'enseignement et de recherche français ou étrangers, des laboratoires publics ou privés.

A zebrafish model of *Mycobacterium kansasii* infection reveals large extracellular cord formation

Matt D. Johansen[1] and Laurent Kremer[1, 2 #]

[1] Institut de Recherche en Infectiologie de Montpellier, Centre National de la Recherche Scientifique UMR 9004, Université de Montpellier, Montpellier, France

[2] INSERM, Institut de Recherche en Infectiologie de Montpellier, Montpellier, France

[#]To whom correspondence should be addressed:

Tel: (+33) 4 34 35 94 47; E-mail: laurent.kremer@irim.cnrs.fr

Running title: *Mycobacterium kansasii* cords *in vivo*

Abstract (100 words)

Mycobacterium kansasii is a slow-growing non-tuberculous mycobacteria responsible for co-infections particularly in patients with human immunodeficiency virus. To date, our knowledge of *M. kansasii* infection has been hampered due to the lack of an effective animal model to study pathogenesis. Here, we show the zebrafish embryo is permissive to *M. kansasii* infection, causing a chronic infection and forming granulomas. Upon macrophage depletion, we identified *M. kansasii* forms extracellular cords, resulting in acute infection and rapid larval death. These findings highlight the feasibility of zebrafish to study *M. kansasii* pathogenesis, and for the first time identify extracellular cords in this species.

Keywords: *Mycobacterium kansasii*, granuloma, infection, cords, zebrafish, macrophage

Background (2000 words)

Mycobacterium kansasii is a slow-growing photochromogenic non-tuberculous mycobacteria (NTM). This opportunistic pathogen is a common source of severe pulmonary infections in patients with human immunodeficiency virus (HIV), chronic obstructive pulmonary disorder and generalised immunosuppression [1-3]. It is regarded as one of the phylogenetically closest species to *Mycobacterium tuberculosis* and is clinically indistinguishable based on clinical symptoms and radiographic features [2]. Previous research has reported >50% mortality rates in patients with HIV and *M. kansasii* co-infections [1], representing a significant public health burden in at-risk populations.

Despite the significance of *M. kansasii* infections in specific patient subpopulations, there has been very little research exploring pathogenicity of this species. Previous reports demonstrated that type I *M. kansasii* ATCC 12478 is able to rupture the phagosomal membrane similarly to *M. tuberculosis* [4], yet it is only able to cause a persistent non-replicating infection in a murine model [2]. As such, there is an urgent need to explore alternative animal models to study *M. kansasii* pathogenesis. In recent years, the zebrafish has emerged as an important infection model to investigate mycobacterial infections, recapitulating important aspects of the human mycobacterial infection, such as granuloma formation [5-7]. Advancements in genetics have allowed the generation of fluorescently labelled cellular subsets and zebrafish knockout lineages, allowing us to explore specific determinants of host immunity [8]. In particular, the zebrafish embryo is optically transparent and possesses a functional innate immune response from approximately 30 hours post-fertilisation, allowing the visualisation of early host-pathogen interactions at the cellular level [7, 8]. Therefore, we explored whether zebrafish embryos could be used as a model for *M. kansasii* infection and examined initial host-pathogen interactions.

Methods

Bacterial culture and generation of fluorescent *M. kansasii*

M. kansasii ATCC 12478 and *M. marinum* M strain (ATCC BAA-535) were grown in Middlebrook 7H9 broth (BD Difco) and supplemented with 0.025% Tyloxapol and 10% oleic acid, albumin, dextrose, catalase (OADC enrichment) ($7H9^{OADC/T}$) or on Middlebrook 7H10 agar (BD Difco) containing 10% OADC enrichment ($7H10^{OADC}$). Bacteria were cultured at 37°C unless otherwise indicated. Antibiotics were included where required for fluorescent strains.

Fluorescent *M. kansasii* was generated using pTEC15 and pTEC27 (a gift from Lalita Ramakrishnan) as previously described [9], however $7H9^{OADC/T}$ was used instead of Sauton's and all incubation and wash steps were completed at 37°C and not 4°C. For selection of fluorescent colonies, *M. kansasii* was plated on $7H10^{OADC}$ containing 50 µg/mL hygromycin (Euromedex). Positive colonies were selected based on fluorescence and maintained in $7H9^{OADC/T}$ supplemented with 50 µg/mL hygromycin. Fluorescent *M. marinum* M strain has been previously described [10].

Zebrafish maintenance and infection

Zebrafish experiments were completed in accordance with the Comité d'Ethique pour l'Expérimentation Animale de la Région Languedoc Roussillon under the reference CEEALR36-1145. Experiments were performed using the *golden* mutant and macrophage reporter Tg(*mpeg1:mCherry)* line, as previously described [6]. Single cell bacterial preparations were completed as previously described [6] and used immediately and not from frozen stocks. Zebrafish caudal vein injections and lipoclodronate macrophage depletion were conducted, as reported [6]. Following infection, embryo age is expressed as days post-infection

(dpi). Embryo survival was monitored daily based on the presence of a heartbeat. For live imaging, zebrafish embryos were anaesthetised in 0.02% tricaine solution [6, 10], mounted on 3% (w/v) methylcellulose and imaged using a Zeiss Axio Zoom.V16 coupled with an Axiocam 503 mono (Zeiss). Fluorescence Pixel Count (FPC) measurements were determined using the 'Analyse particles' function in ImageJ and normalised for each experiment against the corresponding control. All experiments were completed at least three times independently.

Statistical analysis

Survival curve analysis was completed using the log-rank (Mantel-Cox) statistical test. Cord, granuloma and bacterial burden (FPC) analysis were completed using unpaired Student's *t*-test. All statistical tests were completed using Graphpad Prism (Version 8.0.1).

Results

***Mycobacterium kansasii* infection causes a chronic infection in zebrafish embryos**

A critical characteristic of zebrafish manipulation is the requirement for lower ambient temperatures of 28.5°C. As such, we first determined whether *M. kansasii* can replicate at lower temperatures compared to traditional 37°C incubation. We found that *M. kansasii* is able to grow and replicate at 30°C, albeit slower than at 37°C which was to be expected as for other NTM species [6] (**Supplementary Figure 1**).

Previous research has demonstrated that the zebrafish embryo is an attractive model organism for mycobacterial pathogens such as *M. marinum* and *M. abscessus* and recapitulating important pathophysiological hallmarks of human mycobacterial infection and leading to larval death [6, 7]. With this in mind, we wanted to determine whether *M. kansasii* was able to promote larval death in a dose-dependent manner. We found that *M. kansasii*

resulted in ≤10% embryo mortality in a 12-day period, irrespective of infectious dose. Comparatively, *M. marinum*, which is an important fish and human pathogen, led to 100% embryo mortality within 9 dpi (**Figure 1A**), as previously reported [7].

We next wanted to explore whether *M. kansasii* ATCC 12478 is rapidly cleared following infection, or whether it causes a persistent infection. Using live whole embryo fluorescent imaging, we observed the formation of granulomas in 50-60% of embryos from 3 dpi onwards (**Figure 1B-D**). Moreover, when we examined the average number of granulomas per infected embryo over time, we observed a trend for the increasing number of granulomas between 3 and 9 dpi, however this was not significant ($P = 0.06$) (**Supplementary figure 2**). Overall, these results highlight that the zebrafish embryo is permissive to *M. kansasii* infection, leading to a chronic infection characterised by granuloma formation.

Mycobacterium kansasii is able to form large extracellular cords and resist phagocytosis

Macrophages are important immune cells recruited to an infection and are the predominant cell subset within the mycobacterial granuloma [7, 11]. Previous work showed that macrophage ablation results in rapid larval death within several days of infection, underpinning the crucial role of these phagocytes in containing mycobacterial infections [6, 12]. Thus, we explored whether macrophages are responsible for *M. kansasii* infection control. Following liposomal clodronate treatment, which depletes macrophages until approximately 6 days post-treatment (**Supplementary figure 3**), we observed progressive larval death resulting in ~70% of dead embryos at 12 dpi as compared to standard *M. kansasii* infection or following liposomal PBS injection prior to infection (**Figure 2A)**. When we examined the bacterial burden in clodronate-treated embryos, there was a significant increase from 2 dpi onwards when compared to wild-type infections (**Figure 2B**).

Using whole embryo live fluorescent imaging in clodronate-treated embryos, we identified the presence of large extracellular cords in 20% of embryos from 3 dpi, which increased to >80% by 9 dpi (**Figure 2C**). Comparatively, extracellular cord formation in wild-type embryos was a rare event, occurring in <10% of infected embryos and only at 9 dpi (**Figure 2C**). When we further categorised the proportion of cords per embryo, we identified a progressive increase in the number of moderate (6-10 cord/embryo) and heavy (>10 cords/embryo) number of cords up to 9 dpi, as compared to 3 dpi in which 100% of corded embryos had a low number of cords (1-5 cords/embryo) (**Figure 2C**). Following macrophage repopulation at 6 days post clodronate-treatment, we observed the gradual recruitment of macrophages to extracellular cords at approximately 9 dpi (**Figure 2D**). However, based on the sheer size of these observed cords in comparison to the size of the recruited macrophages, they were unable to degrade or control cord formation, in agreement with the increase in the number of embryos with cords and the average number of cords (**Figure 2C**). Finally, to determine if cord formation is an acquired *in vivo* phenotype of *M. kansasii*, we examined stationary-phase liquid cultures for the presence of cords. Using fluorescent microscopy, we observed the presence of large bacterial aggregates resembling cords, demonstrating that this is an intrinsic *M. kansasii* phenotype (**Supplementary Figure 4**).

Collectively, these findings highlight the critical role of macrophages in the control of *M. kansasii* infection and preventing the formation of large extracellular cords. Importantly, to our knowledge this is the first reported observation of *M. kansasii* cord formation both *in vitro* and *in vivo,* which has significant implications for our understanding of *M. kansasii* pathogenesis.

Discussion

In this study, we report for the first time the applicability of the zebrafish embryo to study the pathogenesis of *M. kansasii*. Using this model organism, we demonstrate that under standard infection conditions, a type I *M. kansasii* strain causes a persistent and replicating infection typified by the presence of mycobacterial granulomas. Most importantly, we report here that *M. kansasii* forms large extracellular cords, representing a significant pathogenic trait of this NTM that was previously unexplored.

In recent years, the zebrafish model has established itself as a revolutionary platform to examine host-pathogen interactions in real-time [7, 8]. Using this to our advantage in the current study, we were able to monitor the kinetics of granuloma formation following *M. kansasii* infection which revealed a chronic *in vivo* phenotype, representative of other slow-growing mycobacteria, including *M. tuberculosis*. It is notable that the zebrafish embryo does not possess adaptive immunity until later developmental stages and as such, the role of adaptive immunity in *M. kansasii* remains unexplored. However, adult zebrafish have fully functional innate and adaptive immunity and may be a feasible model organism to examine the role of complete immunity of *M. kansasii* infection in subsequent studies.

Cord formation is a pathophysiological hallmark of acute mycobacterial disease [6, 13-15]. Following the successful escape from the phagosome, mycobacteria such as *M. abscessus*, *M. marinum* and *M. tuberculosis* [4], are able to grow extracellularly as large cords which vastly exceed the size of recruited immune cells and ultimately resist phagocytosis [6]. To date, this phenotypic characteristic has only been identified within a few pathogenic mycobacteria species and has often been reserved for those that have been considered most virulent. We report here, the formation of large extracellular cords in *M. kansasii* both *in vitro* and *in vivo*. That *M. kansasii* shares this phenotypic trait with *M. tuberculosis* further supports the recent

view that *M. kansasii* is an environmental ancestor of *M. tuberculosis* and can be used as a model organism to investigate the transition from an environmental opportunistic pathogen to a host-restricted pathogen [2]. Following macrophage depletion, we observed a large increase in the presence and abundance of cords, highlighting the importance of macrophages in *M. kansasii* infection. Severe infections with *M. kansasii* are often associated with co-existing infections such as HIV, suggesting that immunodeficiency is an important risk factor in the severity of *M. kansasii* infection [3]. Consequently, our observations of extensive cord formation following macrophage ablation may be viewed as clinically relevant and may provide an explanation for the higher mortality rate associated with *M. kansasii* co-infection in immunocompromised patients. As this is the first report of cord formation in *M. kansasii*, it is important that subsequent studies examine the role of cord formation in clinical isolates and screen patient sputum for the presence of *M. kansasii* extracellular cords to support these observations.

While cording in wild-type embryos can be considered a rare event in the context of the current study, it is not entirely absent suggesting that *M. kansasii* can eventually escape from the phagosome. This observation fits with previous work which has identified that *M. kansasii* is able to rupture the phagosomal membrane, indicative of phagosomal escape [2, 4]. Moreover, *M. kansasii* has been demonstrated to secrete esxA and esxB; two effector proteins of the well-characterised ESX-1 locus, which are known to assist in phagosomal escape for *M. marinum* and *M. tuberculosis* [2]. However, to date, the role of ESX-1 in *M. kansasii* pathogenesis remains to be explored.

In summary, our findings highlight the applicability of the zebrafish embryo to examine host-pathogen interactions and pathogenesis for the study of *M. kansasii*. Furthermore, using our new animal model, we have demonstrated that *M. kansasii* causes a chronic infection which is largely controlled by patrolling macrophages in a wild-type infection. Most importantly, we

209 have shown that *M. kansasii* forms large cords both *in vitro* and *in vivo*, ultimately representing
210 a previously unexplored virulence trait of this clinically significant NTM species.

211

212 **Funding**

213 MDJ received a post-doctoral fellowship granted by Labex EpiGenMed, an «Investissements
214 d'avenir» program (ANR-10-LABX-12-01).

215

216 **Conflicts of interest**

217 The authors have no conflict of interest to declare.

218

219 **Figure legends**

220 **Figure 1: *Mycobacterium kansasii* induces a chronic infection in zebrafish.** (A) Zebrafish
221 embryos at approximately 30 hours post-fertilisation were infected with increasing doses of *M.*
222 *kansasii* ATCC 12478, or 100 CFU of *M. marinum* M strain *via* caudal vein injection and
223 survival was monitored over a 12-day period. Each group consists of approximately 20
224 embryos, with each experiment completed at least three independent times. Statistical
225 significance was determined using the log-rank (Mantel Cox) test. **(B)** The proportion of
226 infected zebrafish embryos with granulomas detected *via* fluorescent microscopy at 3, 6 and 9
227 days post-infection (dpi). Each experiment was completed three independent times, with
228 approximately 20 embryos per group. Error bars represent standard deviation. Statistical
229 analysis was completed using the Student's *t*-test. **(C)** Example image of granulomas located
230 in the trunk region of zebrafish embryos infected with *M. kansasii* at 9 dpi. Macrophages are
231 labelled in red, while *M. kansasii* is labelled in green. Granulomas are highlighted with white
232 arrows. Scale bar represents 1 mm. **(D)** Representative image of several macrophages (red)

infected with *M. kansasii* (green) forming a granulomatous infection foci at 9 dpi. Scale bar represents 100 µm.

Figure 2: Macrophages are critical determinants of host immunity to *M. kansasii* infection and prevent extracellular cord formation. (A) Zebrafish embryos at 24 hours post-fertilisation were injected with lipoclodronate *via* caudal vein injection to deplete macrophages. Following 6 hours treatment, embryos were infected with 300 CFU *M. kansasii* ATCC 12478 *via* caudal vein injection and survival was monitored daily over a 12-day period. Statistical significance was determined using the log-rank (Mantel Cox) test. **(B)** Bacterial burden was quantified by fluorescent pixel counts (FPC) using ImageJ, with each point representing an individual embryo. Error bars represent standard deviation. Statistical analysis was completed using the Student's *t*-test. **(C)** The proportion of infected zebrafish embryos with extracellular cords detected (left panel) and the average number of cords per embryo split into low (1-5 cords/embryo), moderate (6-10 cords/embryo) and high (>10 cords/embryo) number of cords per embryo (right panel) that were detected using fluorescent microscopy at 3, 6 and 9 days post-infection (dpi). The number of embryos analysed is indicated into brackets. Error bars represent standard deviation. Statistical analysis was completed using Student's *t*-test. **(D)** Representative images of extracellular cords identified using whole embryo live fluorescent microscopy on the trunk region at 6 dpi (left panel) and 9 dpi (right panel). Macrophages are labelled in red and *M. kansasii* is labelled in green. Cords are highlighted with white arrows. Scale bars represent 1 mm and 100 µm, respectively. *** $P \leq 0.001$, **** $P \leq 0.0001$. ns, non-significant.

Supplementary Figure 1: *M. kansasii* is able to replicate at lower temperatures. *M. kansasii* ATCC 12478 was inoculated in $7H9^{OADC/T}$ at an optical density of 0.05 (OD_{620}) and

incubated at 30°C and 37°C under shaking at 100 rpm. Growth measurements were taken daily over a 16-day period until cultures reached stationary phase.

Supplementary Figure 2: Aaverage numbers of granulomas per embryo over time. Macrophage reporter embryos Tg(*mpeg1:mCherry)* at approximately 30 hours post-fertilisation were infected with 300 CFU of *M. kansasii* ATCC 12478 *via* caudal vein injection. The average number of granulomas per infected zebrafish embryos was detected *via* fluorescent microscopy at 3, 6 and 9 days post-infection (dpi). Each experiment was completed three independent times, with approximately 20 embryos per group. Error bars represent standard deviation. Statistical analysis was completed using the Student's *t*-test.

Supplementary figure 3: Efficacy of liposomal clodronate macrophage depletion and restoration kinetics. Macrophage reporter embryos Tg(*mpeg1:mCherry)* at 24 hours post-fertilisation were injected with either PBS clodronate or liposomal clodronate *via* caudal vein injection to deplete macrophages (in red). Following 6 hours treatment, embryos were infected with 300 CFU *M. kansasii* ATCC 12478 (in green). Embryos were monitored at 3 and 6 dpi to determine the rate of regeneration of macrophages in treated embryos. Scale bars represent 1mm.

Supplementary Figure 4: *M. kansasii* forms large bacterial cords under standard *in vitro* culture conditions. *M. kansasii* ATCC 12478 was inoculated in $7H9^{OADC/T}$ at an optical density of 0.05 (OD_{620}) and incubated at 37°C with no agitation for approximately 2 weeks, after which bacteria were mounted onto a glass slide and visualised using fluorescent microscopy. Scale bars presents 50 µm.

References

1. Marras TK, Morris A, Gonzalez LC, Daley CL. Mortality prediction in pulmonary *Mycobacterium kansasii* infection and human immunodeficiency virus. Am J Respir Crit Care Med **2004**; 170:793-8.

2. Wang J, McIntosh F, Radomski N, *et al*. Insights on the emergence of *Mycobacterium tuberculosis* from the analysis of *Mycobacterium kansasii*. Genome Biol Evol **2015**; 7:856-70.

3. Lovell JP, Zerbe CS, Olivier KN, *et al*. Mediastinal and disseminated *Mycobacterium kansasii* disease in GATA2 deficiency. Ann Am Thorac Soc **2016**; 13:2169-73.

4. Houben D, Demangel C, van Ingen J, *et al*. ESX-1-mediated translocation to the cytosol controls virulence of mycobacteria. Cell Microbiol **2012**; 14:1287-98.

5. Madigan CA, Cameron J, Ramakrishnan L. A zebrafish model of *Mycobacterium leprae* granulomatous infection. J Infect Dis **2017**; 216:776-9.

6. Bernut A, Herrmann J-L, Kissa K, *et al*. *Mycobacterium abscessus* cording prevents phagocytosis and promotes abscess formation. Proc Nat Acad Sci USA **2014**; 111:943-52.

7. Davis JM, Clay H, Lewis JL, Ghori N, Herbomel P, Ramakrishnan L. Real-time visualization of mycobacterium-macrophage interactions leading to initiation of granuloma formation in zebrafish embryos. Immunity **2002**; 17:693-702.

8. Cronan MR, Tobin DM. Fit for consumption: zebrafish as a model for tuberculosis. Dis Model Mech **2014**; 7:777-84.

9. Viljoen A, Gutierrez AV, Dupont C, Ghigo E, Kremer L. A simple and rapid gene disruption strategy in *Mycobacterium abscessus*: On the design and application of glycopeptidolipid mutants. Front Cell Infect Microbiol **2018**; 8:69.

10. Takaki K, Davis JM, Winglee K, Ramakrishnan L. Evaluation of the pathogenesis and treatment of *Mycobacterium marinum* infection in zebrafish. Nat Protoc **2013**; 8:1114-24.

11. Ramakrishnan L. Revisiting the role of the granuloma in tuberculosis. Nature Reviews Immunology **2012**; 12:352-66.

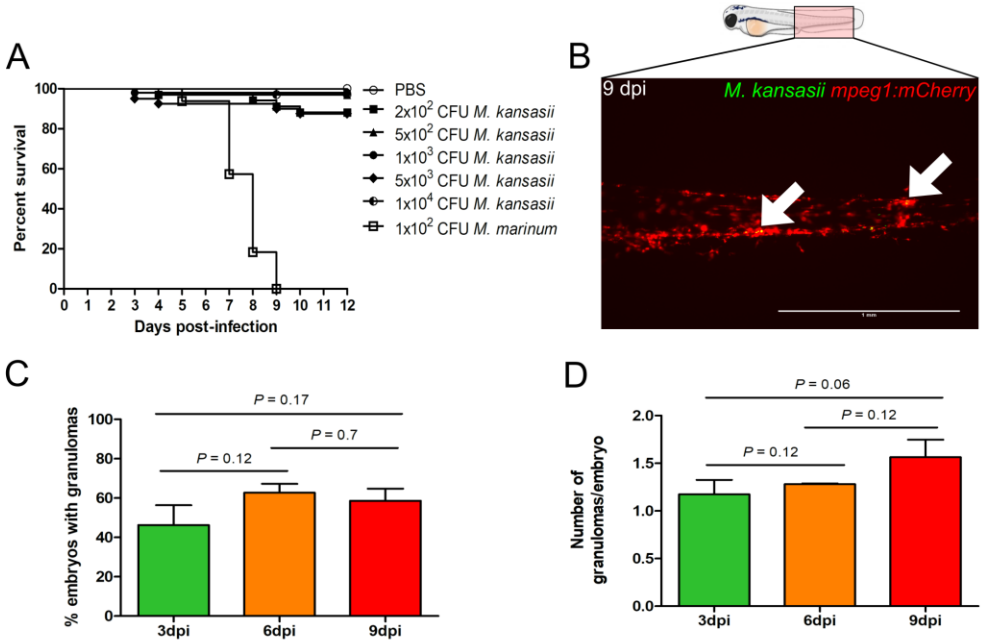
12. Clay H, Davis JM, Beery D, Huttenlocher A, Lyons SE, Ramakrishnan L. Dichotomous role of the macrophage in early *Mycobacterium marinum* infection of the zebrafish. Cell Host Microbe **2007**; 2:29-39.

13. Julian E, Roldan M, Sanchez-Chardi A, Astola O, Agusti G, Luquin M. Microscopic cords, a virulence-related characteristic of *Mycobacterium tuberculosis*, are also present in nonpathogenic mycobacteria. J Bacteriol **2010**; 192:1751-60.

14. Sanchez-Chardi A, Olivares F, Byrd TF, Julian E, Brambilla C, Luquin M. Demonstration of cord formation by rough *Mycobacterium abscessus* variants: implications for the clinical microbiology laboratory. J Clin Microbiol **2011**; 49:2293-5.

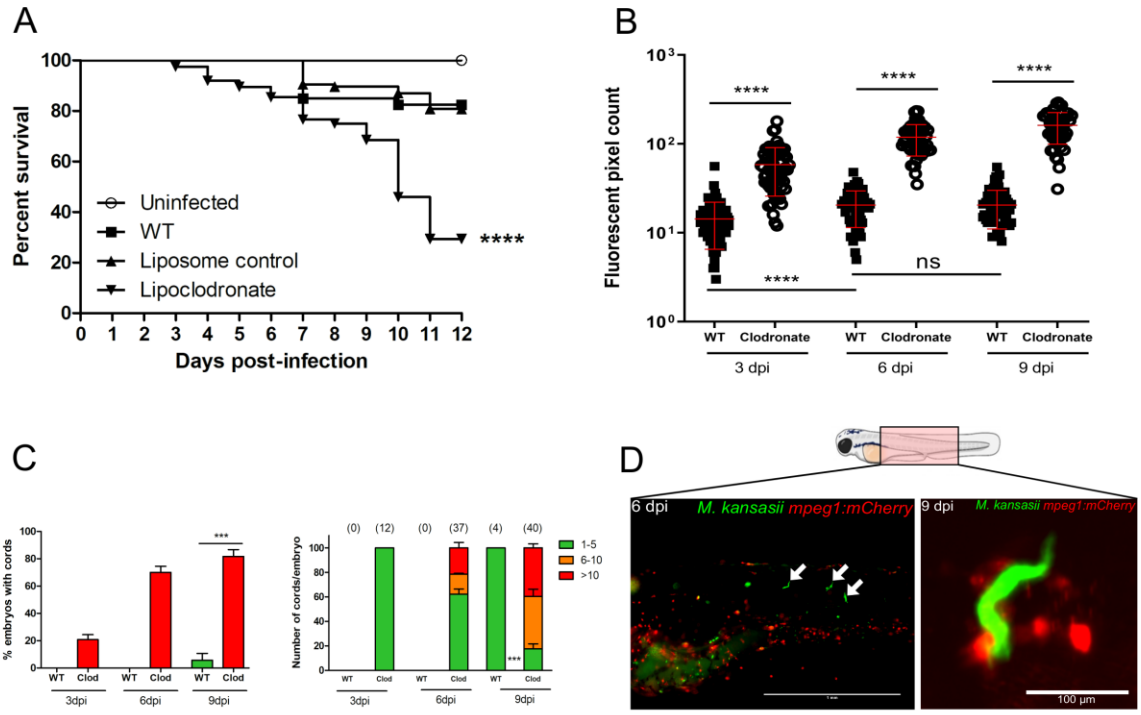
15. Middlebrook G, Dubos RJ, Pierce C. Virulence and morphological characteristics of mammalian tubercle bacilli. J Exp Med **1947**; 86:175-84.

333


A
Percent survival
Days post-infection
PBS
2x10^2 CFU M. kansasii
5x10^2 CFU M. kansasii
1x10^3 CFU M. kansasii
5x10^3 CFU M. kansasii
1x10^4 CFU M. kansasii
1x10^2 CFU M. marinum
B
9 dpi
M. kansasii mpeg1:mCherry
C
% embryos with granulomas
P = 0.17
P = 0.7
P = 0.12
3dpi
6dpi
9dpi
D
Number of granulomas/embryo
P = 0.06
P = 0.12
P = 0.12
3dpi
6dpi
9dpi

334

335


A
Percent survival
Days post-infection
Uninfected
WT
Liposome control
Lipoclodronate
****
B
Fluorescent pixel count
WT
Clodronate
3 dpi
6 dpi
9 dpi
ns
C
% embryos with cords
Number of cords/embryo
3dpi
6dpi
9dpi
1-5
6-10
>10
D
6 dpi
M. kansasii mpeg1:mCherry
9 dpi
100 µm